0026-895X/06/6904-1413–1420$20.00
MOLECULAR PHARMACOLOGY
Copyright © 2006 The American Society for Pharmacology and Experimental Therapeutics
Mol Pharmacol 69:1413–1420, 2006

Vol. 69, No. 4
21154/3098070
Printed in U.S.A.

A Pyrazole Derivative Potently Inhibits Lymphocyte Ca^{2+} Influx and Cytokine Production by Facilitating Transient Receptor Potential Melastatin 4 Channel Activity

Ryuichi Takezawa, Henrique Cheng, Andreas Beck, Jun Ishikawa, Pierre Launay, Hirokazu Kubota, Jean-Pierre Kinet, Andrea Fleig, Toshimitsu Yamada, and Reinhold Penner

Laboratory of Cell and Molecular Signaling, Center for Biomedical Research at the Queen's Medical Center and John A. Burns School of Medicine at the University of Hawaii, Honolulu, Hawaii (H.C., A.B., A.F., R.P.); Inflammation Research, Pharmacology Laboratories (R.T., J.I., T.Y.), Medicinal Chemistry Research II, Chemistry Laboratories (H.K.), Institute for Drug Discovery Research, Astellas Pharma Inc., Tsukuba, Ibaraki, Japan; and Department of Pathology, Beth Israel Deaconess Medical Center and Harvard Medical School, Boston, Massachusetts (P.L., J.-P.K.)

Received November 24, 2005; accepted January 10, 2006

ABSTRACT

3,5-Bis(trifluoromethyl)pyrazole derivative (BTP2) or *N*-[4–3,5-bis(trifluromethyl)pyrazol-1-yl]-4-methyl-1,2,3-thiadiazole-5-carboxamide (YM-58483) is an immunosuppressive compound that potently inhibits both Ca^{2+} influx and interleukin-2 (IL-2) production in lymphocytes. We report here that BTP2 dose-dependently enhances transient receptor potential melastatin 4 (TRPM4), a Ca^{2+}-activated nonselective (CAN) cation channel that decreases Ca^{2+} influx by depolarizing lymphocytes. The effect of BTP2 on TRPM4 occurs at low nanomolar concentrations and is highly specific, because other ion channels in T lymphocytes are not significantly affected, and the major Ca^{2+} influx pathway in lymphocytes, I_{CRAC}, is blocked only at 100-fold higher concentrations. The efficacy of BTP2 in blocking IL-2 production is reduced approximately 100-fold when preventing TRPM4-mediated membrane depolarization, suggesting that the BTP2-mediated facilitation of TRPM4 channels represents the major mechanism for its immunosuppressive effect. Our results demonstrate that TRPM4 channels represent a previously unrecognized key element in lymphocyte Ca^{2+} signaling and that their facilitation by BTP2 supports cell membrane depolarization, which reduces the driving force for Ca^{2+} entry and ultimately causes the potent suppression of cytokine release.

In many cells, receptor activation evokes an increase in cytosolic Ca^{2+} concentration ($[Ca^{2+}]_i$) composed of release from intracellular stores followed by store-operated Ca^{2+} entry via calcium release-activated calcium (CRAC) channels (Penner et al., 1993; Parekh and Penner, 1997; Putney et al., 2001). These channels are functionally best characterized in mast cells (Hoth and Penner, 1992, 1993) and T lymphocytes (Zweifach and Lewis, 1993; Premack et al., 1994) and are considered key elements for the activation of immune cells. The study of CRAC has been hampered by the lack of potent and specific pharmacological tools. At present, the most widely used organic blockers of store-operated calcium entry pathways are imidazole antimycotics, such as econazole, the closely related compound SKF-96365, and 2-aminoethoxydiphenyl borate (Mason et al., 1993; Chung et al., 1994; Franzius et al., 1994; Christian et al., 1996; Hermosura et al., 2002). However, none of these compounds is very potent or selective.

A class of pyrazole derivatives, bis(trifluoromethyl)pyrazoles (BTPs), has been reported to act as potent immuno-

This work was supported in part by the following grants from the National Institutes of Health: R01-AI50200, R01-GM63954, and R01-NS40927 (to R.P.); R01-GM65360 (to A.F.); and R01-AI46734 (to J.-P.K.). P.L. was supported by a fellowship from Human Frontier Science Program Organization.

Article, publication date, and citation information can be found at http://molpharm.aspetjournals.org.

doi:10.1124/mol.105.021154.

ABBREVIATIONS: CRAC, calcium release-activated calcium (channel); TRP, transient receptor potential; TRPM4, transient receptor potential melastatin 4; BTP, bis(trifluoromethyl)pyrazole; BTP2, 3,5-bis(trifluoromethyl)pyrazole derivative; YM-58483, *N*-[4–3,5-bis(trifluromethyl)pyrazol-1-yl]-4-methyl-1,2,3-thiadiazole-5-carboxamide; FBS, fetal bovine serum; IL, interleukin; CAN, Ca^{2+}-activated nonselective; HEK, human embryonic kidney; BAPTA, 1,2-bis(2-aminophenoxy)ethane-*N*,*N*,*N*′,*N*′-tetraacetic acid; PHA, phytohemagglutinin; ELISA, enzyme-linked immunosorbent assay; $InsP_3$, inositol trisphosphate; I-V, current/voltage; SKF-96365, 1-[*β*-[3-(4-methoxyphenyl)propoxy]-4-methoxyphenethyl]-1*H*-imidazole hydrochloride.

suppressive compounds by inhibiting cytokine release (IL-2, IL-4, IL-5, interferon-γ, and others) from human lymphocytes and suppressing T-cell proliferation (Djuric et al., 2000; Trevillyan et al., 2001; Chen et al., 2002; Ishikawa et al., 2003). In addition, these compounds have proven effective in various immune disease-relevant rodent and nonhuman primate models, in which they inhibit trinitrochlorobenzene-induced contact hypersensitivity in mice (a model of T lymphocyte-mediated delayed type hypersensitivity) and *Ascaris suum*-induced immediate bronchoconstriction of cynomolgus monkeys (an asthma model) (Djuric et al., 2000; Ishikawa et al., 2003). Despite the rather detailed characterization of the compound's potent effects in many immune-based cellular and animal models, the mechanism by which BTPs inhibit cytokine production in lymphocytes remains unknown. The effects of BTPs are presumably linked to intracellular Ca^{2+} signaling, because the pyrazole derivative BTP2 (Fig. 2D) potently inhibits thapsigargin-evoked Ca^{2+} influx in the low nanomolar range (Ishikawa et al., 2003), and two recent reports suggest that BTP2 may inhibit the store-operated Ca^{2+} current I_{CRAC} (Zitt et al., 2004; He et al., 2005) and TRPC3 and TRPC5 channels (He et al., 2005).

The transient receptor potential (TRP) proteins represent an important family of mammalian ion channels that are believed to be involved in Ca^{2+} signaling. Based on sequence similarities, the mammalian TRP channel family is divided into three subfamilies: TRPC, TRPV, and TRPM (Harteneck et al., 2000; Clapham et al., 2001; Montell et al., 2002a,b). TRPM4, specifically the longer splice variant TRPM4b (which we will refer to as TRPM4 throughout this manuscript), is a widely expressed Ca^{2+}-activated nonselective cation channel of the TRPM ion channel subfamily that does not conduct Ca^{2+} but instead mediates cell membrane depolarization (Launay et al., 2002). In electrically nonexcitable cells, a depolarization would tend to decrease the driving force for Ca^{2+} influx through store-operated Ca^{2+} channels. Many other ion channels, such as voltage-dependent potassium (Kv1.3) channels (Lin et al., 1993; Hanson et al., 1999), intermediate/small-conductance calcium-activated potassium (IK/SK2) channels (Lin et al., 1993; Jensen et al., 1999; Desai et al., 2000; Wulff et al., 2000), and swelling-activated chloride (Cl_{vol}) channels (Lewis et al., 1993; Ross et al., 1994), are also known to be involved in the regulation of the driving force for Ca^{2+} influx, but they do so by hyperpolarizing the membrane potential (Penner et al., 1988; Cahalan and Chandy, 1997; Cahalan et al., 2001). Thus, the net Ca^{2+} influx into a cell is not only determined by Ca^{2+} entry pathways themselves, but also by ion channels that modulate the membrane potential.

In the present study, we investigated the mechanism by which BTP2 inhibits Ca^{2+} signaling in Jurkat T cells. We demonstrate that BTP2 potently and selectively facilitates the activity of TRPM4, resulting in reduced Ca^{2+} entry and cytokine release. This compound therefore represents a novel and promising pharmacological tool to inhibit Ca^{2+} signaling in lymphocytes and other cell types that regulate Ca^{2+} influx by the concerted actions of store-operated Ca^{2+} channels and Ca^{2+}-activated cation channels.

Materials and Methods

Cells. HEK-293 cells transfected with the FLAG-human TRPM4b/pCDNA4/TO construct were grown on glass coverslips with Dulbecco's modified Eagle's medium supplemented with 10% FBS, blasticidin (5 μg/ml), and zeocin (0.4 mg/ml). TRPM4b expression was induced 1 day before use by adding 1 μg/ml tetracycline to the culture medium, and patch-clamp experiments were performed 16 to 24 h after induction (for details, see Launay et al., 2002). Human leukemic T cells (Jurkat cells) were grown in RPMI 1640 medium (10% FBS) and rat basophilic leukemia cells (RBL-2H3 cells) in Dulbecco's modified Eagle's medium (10% FBS).

Materials. BTP2 (or YM-58483) and SKF-96365 were synthesized by Astellas Pharma Inc. (Tokyo, Japan). Econazole, margatoxin, apamin, charybdotoxin, and stilbenedisulfonate 4,4-diisothiocyanatostilbene-2,2′-disulfonic acid were purchased from Sigma and dissolved in dimethyl sulfoxide. Phytohemagglutinin (PHA) was obtained from Sigma (St. Louis, MO) and dissolved in phosphate-buffered saline.

Solutions. For I_{CRAC} measurements, the standard bath solution had the following composition: 140 mM NaCl, 2.8 mM KCl, 10 mM $CaCl_2$, 2 mM $MgCl_2$, 10 mM CsCl, 10 mM glucose, and 10 mM HEPES·NaOH, pH 7.2, with osmolarity adjusted to approximately 320 mOsM. Intracellular pipette-filling solutions contained 140 mM cesium glutamate, 8 mM NaCl, 1 mM $MgCl_2$, 10 mM cesium-BAPTA, and 10 mM HEPES·CsOH, pH 7.2, adjusted with CsOH. In experiments in which $[Ca^{2+}]_i$ was buffered to elevated levels, $CaCl_2$ was added as necessary [calculated with WebMaxC (http://www.stanford.edu/~cpatton/webmaxcS.htm), temperature = 24°C, pH = 7.2, ionic equivalent = 0.16]. Solution changes were performed by pressure ejection from a wide-tipped pipette.

Electrophysiology. Patch-clamp experiments were performed in the tight-seal whole-cell configuration at 21 to 25°C. High-resolution current recordings were acquired by a computer-based patch-clamp amplifier system (EPC-9; HEKA, Lambrecht, Germany). Patch pipettes had resistances between 2 and 4 MΩ after filling with the standard intracellular solution. Immediately after establishment of the whole-cell configuration, voltage ramps of 50- to 200-ms duration spanning the voltage range of −100 to +100 mV were delivered at a rate of 0.5 Hz over a period of 300 to 400 s. All voltages were corrected for a liquid junction potential of 10 mV between external and internal solutions when using glutamate as an intracellular anion. Currents were filtered at 2.9 kHz and were digitized at 100-μs intervals. Capacitive currents and series resistance were determined and corrected before each voltage ramp using the automatic capacitance compensation of the EPC-9. The low-resolution temporal development of membrane currents was assessed by extracting the current amplitude at −80 or +80 mV from individual ramp current records. Where applicable, statistical errors of averaged data are given as means ± S.E.M. with n determinations.

Voltage-dependent potassium (Kv1.3) currents were measured in Jurkat cells. The bath solution contained 160 mM NaCl, 4.5 mM KCl, 2 mM $CaCl_2$, 1 mM $MgCl_2$, and 10 mM HEPES·NaOH, pH 7.2. The internal solution contained 140 mM potassium glutamate, 2 mM $MgCl_2$, 1 mM $CaCl_2$, 10 mM potassium-EGTA, and 10 mM HEPES·KOH, pH 7.2. Ramps were given every 30 s (−100 to +100 mV in 200 ms), and cells were held at −80 mV between ramps. Currents were not leak-subtracted.

Calcium-activated potassium (SK2) currents were measured in Jurkat cells. The bath solution contained 164.5 mM KCl, 2 mM $CaCl_2$, 1 mM $MgCl_2$, and 5 mM HEPES·KOH, pH 7.2. The internal solution contained 135 mM potassium aspartate, 2 mM $MgCl_2$, 1.1 mM potassium EGTA, and 10 mM HEPES·KOH, pH 7.2. Ramps were given every 2 s (−100 to +40 mV in 200 ms), and cells were held at −80 mV between ramps. Free intracellular $[Ca^{2+}]_i$ was adjusted to 1 μM.

Swelling-activated chloride (Cl_{vol}) currents were measured in Jurkat cells. The bath solution contained 160 mM NaCl, 4.5 mM KCl, 1

mM $MgCl_2$, 2 mM $CaCl_2$, and 5 mM HEPES·NaOH, pH 7.2. The internal solution contained 160 mM cesium glutamate, 2 mM $MgCl_2$, 0.1 mM $CaCl_2$, 1.1 mM cesium-EGTA, 4 mM sodium ATP, 100 mM glucose, and 10 mM HEPES·CsOH, pH 7.2. Ramps were given every 2 s (−100 to +50 mV in 200 ms), and cells were held at −60 mV between ramps.

TRPM4 currents were measured in Jurkat and HEK-293 cells overexpressing TRPM4b. The bath solution contained 140 mM NaCl, 2.8 mM KCl, 2 mM $MgCl_2$, 1 mM $CaCl_2$, 10 mM glucose, and 10 mM HEPES·NaOH, pH 7.2. The internal solution contained 120 mM potassium glutamate, 8 mM NaCl, 1 mM $MgCl_2$, 10 mM potassium-BAPTA, and 10 mM HEPES·KOH, pH 7.2. Ramps were given every 2 s (−100 to +100 mV in 50 ms), and cells were held at −80 mV between ramps. Free intracellular $[Ca^{2+}]_i$ was adjusted as indicated in the figure legends.

IL-2 Production Assay. Jurkat cells (5×10^6 cells/ml) were placed in a 96-well microplate and incubated with either 10 μg/ml or 2 μg/ml PHA (Sigma) for 24 h, and the supernatant was collected from these cells after centrifugation (200*g*, 24°C for 3 min). The concentration of IL-2 was measured by the human IL-2 ELISA system (human IL-2 ELISA Kit DuoSet; Genzyme Co., Cambridge, MA). Optical density values at 450 nm were measured with the use of a microplate reader (Spectra Max 190; Molecular Devices, Sunnyvale, CA). Data for BTP2-treated cells were normalized to those of untreated control cells.

Calcium Measurements. For Ca^{2+} measurements, Fura-2 acetoxymethyl ester-loaded cells (5 μM/30 min at 37°C) were kept in standard extracellular saline containing 140 mM NaCl, 2.8 mM KCl, 1 mM $CaCl_2$, 2 mM $MgCl_2$, 10 mM glucose, and 10 mM HEPES·NaOH, pH 7.2, and excited by wavelengths of 340 and 380 nm. Fluorescence emission of several cells was simultaneously recorded at a frequency of 1 Hz using a dual excitation fluorometric imaging system (TILL-Photonics, Gräfelfingen, Germany) controlled by TILL-Vision software. Signals were computed into relative ratio units of the fluorescence intensity of the different wavelengths (340/380 nm).

Results

Effect of BTP2 on I_{CRAC}. Because BTP2 inhibits thapsigargin-induced Ca^{2+} influx (Ishikawa et al., 2003) and reportedly inhibits the store-operated calcium current I_{CRAC} (Zitt et al., 2004), we analyzed the effects of BTP2 on I_{CRAC} in RBL-2H3 and Jurkat T cells. I_{CRAC} was activated by a standard protocol after whole-cell break-in with 20 μM $InsP_3$ in the pipette solution. The time course of whole-cell current was monitored by 200-ms voltage ramps that spanned −100 to +100 mV and were applied every 2 s. Each voltage ramp yields a full current-voltage (I-V) relationship (Fig. 1C), and the I_{CRAC} time course is shown in Fig. 1A. It was constructed by measuring the whole-cell current amplitude on the ramp trace corresponding to −80 mV, normalizing the current amplitude to the value obtained just before the application of compound, and plotting it as a function of time. Extracellularly applied BTP2 blocked $InsP_3$-evoked I_{CRAC} in Jurkat cells in a concentration-dependent manner (Fig. 1A). Complete inhibition of the current was obtained within 200 s after the addition of 10 μM BTP2. Lower concentrations also blocked, but they did so more slowly. Figure 1E shows the dose-response relationship for BTP2-mediated block of I_{CRAC} 300 s after application, along with the dose-response curve obtained for the reference compound econazole under identical experimental conditions (raw data not shown). In Jurkat cells, the apparent IC_{50} values for BTP2 and econazole were 2.2 and 4.0 μM, respectively (Hill coefficient = 1.7 each).

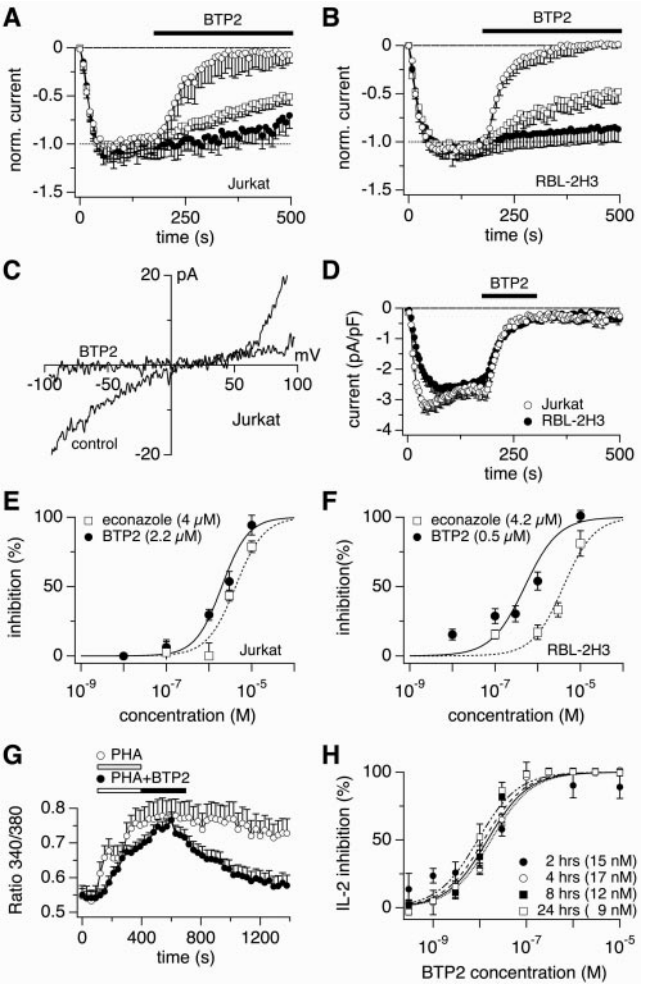

Fig. 1. Effects of BTP2 on I_{CRAC}. Whole-cell currents were recorded in Jurkat cells and RBL-2H3 cells. I_{CRAC} was activated using intracellular solutions containing 20 μM $InsP_3$ and 10 mM BAPTA and was monitored by applying voltage ramps of 50-ms duration that ranged from −100 to +100 mV from a holding potential of 0 mV. Data are ± S.E.M. where applicable. A, average I_{CRAC} at −80 mV (n = 3–10) in Jurkat cells. BTP2 (●, 1 μM; □, 3 μM; ○, 10 μM) was applied extracellularly as indicated by the bar. Currents were normalized to the amplitude at 180 s. B, average I_{CRAC} at −80 mV (n = 3–10) in RBL-2H3 cells. BTP2 (●, 10 nM; □, 1 μM; ○, 10 μM) was applied extracellularly as indicated by the bar. Currents were normalized to the amplitude at 180 s. C, representative I-V relationships for fully activated I_{CRAC} at 180 s and fully inhibited I_{CRAC} (by 10 μM BTP2) at 480 s in Jurkat cells. D, Jurkat and RBL cells were perfused with standard internal solution containing 10 μM BTP2 (n = 10), which failed to block I_{CRAC}. At 180 s into the experiment, 10 μM BTP2 was applied extracellularly and caused complete block of I_{CRAC}. E, dose-response relationship for BTP2- and econazole-mediated block of I_{CRAC} in Jurkat cells (IC_{50} value for BTP2 = 2.2 μM and for econazole = 4.0 μM, with Hill coefficients of 1.7 each). F, dose-response relationship for BTP2- and econazole-mediated block of I_{CRAC} in RBL-2H3 cells (IC_{50} value for BTP2 = 0.5 μM and for econazole = 4.2 μM, with Hill coefficients of 1.4 each). G, average Ca^{2+} signals in intact Jurkat T cells stimulated with PHA (20 μg/ml). Control cells (○, n = 32) produced sustained changes in $[Ca^{2+}]_i$, whereas Ca^{2+} signals in cells that were exposed to 100 nM BTP2 (●, n = 58) returned to baseline within ~10 min. H, dose-response relationships for BTP2-induced inhibition of IL-2 production over different stimulation times. Jurkat cells (5×10^6 cells/ml) were incubated with PHA (10 μg/ml) and various concentrations of BTP2. At the indicated times (range, 2–24 h), IL-2 content in the supernatant was measured by ELISA and normalized to control cells not treated with BTP2 (the absolute amounts of IL-2 in the absence of BTP2 were: 2 h = 9 ± 1.9 pg/ml; 4 h = 135 ± 54 pg/ml; 8 h = 702 ± 157 pg/ml; and 24 h = 1500 ± 329 pg/ml; mean ± S.E.M.).

Next, we studied the effect of BTP2 on I_{CRAC} in RBL-2H3 cells and observed that BTP2 also blocks $InsP_3$-evoked I_{CRAC} in these cells in a concentration-dependent manner (Fig. 1B). With an IC_{50} value of 0.5 μM (Fig. 1F; Hill coefficient = 1.4), BTP2 seems slightly more potent in RBL cells than in Jurkat cells, whereas the potency of econazole in RBL cells (IC_{50} = 4.2 μM; Hill coefficient = 1.4) was similar to that observed in Jurkat cells. To study the site of action, we included BTP2 in the pipette solution. Intracellularly applied BTP2 (10 μM) did not exhibit any inhibitory effect on I_{CRAC} in either RBL-2H3 cells or Jurkat cells, and it did not affect the block of I_{CRAC} induced by extracellularly applied BTP2 in either cell type (Fig. 1D). This suggests that the inhibitory action of BTP2 on I_{CRAC} may be located extracellularly; however, we cannot completely rule out the possibility that the lipophilicity of the compound might allow it to escape rapidly across the plasma membrane before affecting the channel.

Although the above results demonstrate that BTP2 can inhibit I_{CRAC} in both RBL and Jurkat cells, the potency seems to be too low to account for the compound's ability to suppress cytokine production, which occurs in the low nanomolar range. Zitt et al. (2004) reported recently that I_{CRAC} is inhibited by BTP2 at lower concentrations, but this effect requires hours to develop, and they arrived at an IC_{50} value of approximately 10 nM after 24 h of preincubation with the compound (Zitt et al., 2004). He et al. (2005) reported that store-operated Ca^{2+} entry was reduced much quicker, within approximately 10 min, but the concentrations required to do so in HEK-293 cells and DT40 B cells were found to be at least 1 order of magnitude higher (He et al., 2005), similar to the efficacy of BTP2 in blocking I_{CRAC} in RBL cells (Fig. 1F). To further assess the involvement of I_{CRAC}, we analyzed the kinetics of BTP2 action on both Ca^{2+} signaling and cytokine production. Figure 1G illustrates the effect of 100 nM BTP2 on Jurkat Ca^{2+} signals evoked by 10 μg/ml PHA. This relatively low concentration of BTP2 suppressed the PHA-induced Ca^{2+} signals almost completely within approximately 10 min and therefore cannot be reconciled easily with the reported slow I_{CRAC} inhibition (time constant = 98 min) (Zitt et al., 2004). We next analyzed the temporal development of the efficacy of BTP2 to suppress IL-2 release over variable time spans ranging from 2 to 24 h. Jurkat cells were stimulated with 10 μg/ml PHA, and IL-2 production was measured by ELISA at various times after the coapplication of PHA and various concentrations of BTP2. Figure 1H illustrates that there was no significant change in the potency with which BTP2 suppressed IL-2 release, because the IC_{50} value remained constant in the low nanomolar range even when measuring IL-2 release as early as 2 h after stimulation, again suggesting that the main mechanism of action of BTP2 is engaged quickly and does not require several hours to develop. This would suggest that the I_{CRAC} inhibition observed by Zitt et al. (2004) at low nanomolar concentrations may be caused by another event rather than as a direct effect on CRAC channels. Because BTP2 has been demonstrated to suppress lymphocyte proliferation (Trevillyan et al., 2001; Zitt et al., 2004), one possible reason for the decrease in I_{CRAC} amplitude after long BTP2 preincubations could be that lymphocytes become arrested at a certain cell-cycle stage in which I_{CRAC} is suppressed. Indeed, serum-starved RBL cells become arrested in G_0/G_1 and have been reported to lack significant I_{CRAC} (Bodding, 2001). He et al. (2005) found a relatively fast inhibition of store-operated Ca^{2+} influx, but the concentrations required probably reflect the inhibition of I_{CRAC} we observe in, for example, RBL cells. Given that the effect of BTP2 even at low concentrations is relatively quick compared with the time course over which it compromises I_{CRAC}, we considered alternative or additional mechanisms that BTP2 may be targeting.

Effect of BTP2 on Other Ionic Currents in Jurkat Cells. Whole-cell recordings permit the direct measurement of several types of channel activity that may affect Ca^{2+} signaling in Jurkat cells such as the voltage-dependent potassium channel Kv1.3, the small-conductance Ca^{2+}-activated potassium channel SK2, and volume regulatory Cl^- channel Cl_{vol}. We first analyzed the efficacy of known inhibitors of these channels on PHA-stimulated cytokine production in Jurkat T lymphocytes. Of the presumed I_{CRAC} inhibitors, BTP2, econazole, and SKF-96365 (10 μM each), only BTP2 completely inhibited PHA-induced IL-2 production (Fig. 2A), consistent with its complete inhibition of I_{CRAC} at that concentration. Econazole also suppressed cytokine pro-

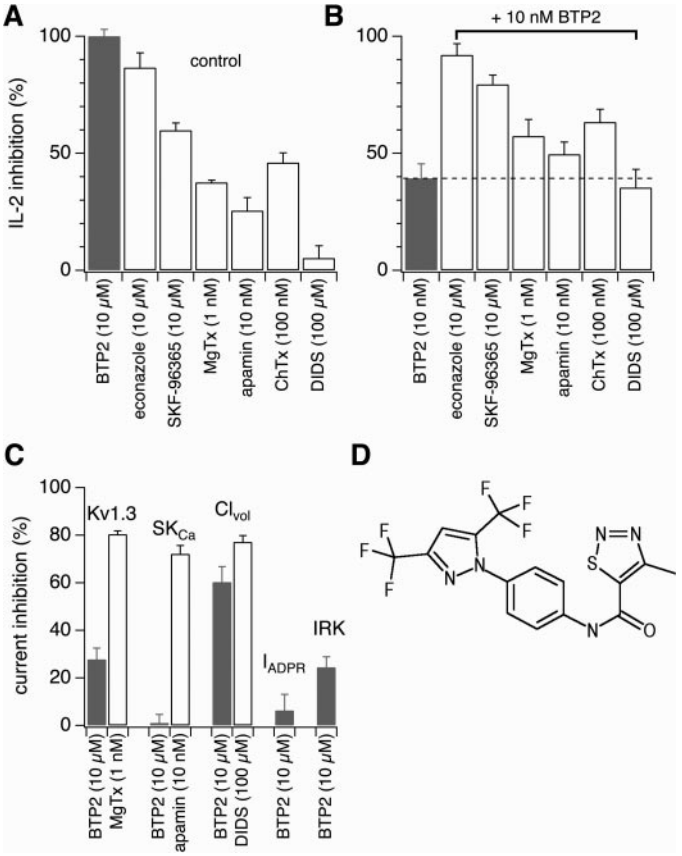

Fig. 2. Effects of channel blockers on IL-2 production and membrane currents in Jurkat cells. Jurkat cells (5×10^6 cells/ml) were incubated with PHA (2 μg/ml). Twenty-four hours after stimulation, IL-2 content in the supernatant was measured by ELISA. Data are ±S.E.M. where applicable. A, effects of different individual channel blockers on IL-2 production (n = 3 each). BTP2 (10 μM) is indicated in gray, and the other compounds are shown as □. B, additive effects of different channel blockers (at the same concentration as in A) on IL-2 production in cells that were treated with 10 nM BTP2 plus the channel blockers (□) compared with 10 nM BTP2 inhibition alone (▨; 10 nM BTP2 caused ~40% inhibition; n = 3 each). For comparison purposes, the broken line indicates the level of inhibition by 10 nM BTP2 alone. C, effects of BTP2 (▨) and reference compounds (□) on different ion channels in Jurkat T cells (n = 5–8). D, chemical structure of BTP2.

duction, albeit not completely, whereas SKF-96365 was not very effective. The other inhibitors exhibited varying degrees of inhibition. The K^+ channel blockers, including the Kv1.3-specific inhibitor margatoxin (1 nM), the SK2 inhibitor apamin (10 nM), and the IK inhibitor charybdotoxin (100 nM), produced inhibitory effects in the range of 30 to 50%, whereas the Cl_{vol} channel inhibitor stilbenedisulfonate 4,4-diisothiocyanatostilbene-2,2′-disulfonic acid (100 μM) was ineffective. The efficacy of K^+ channel blockers to affect IL-2 production is consistent with the fact that they inhibit ion currents which promote Ca^{2+} influx via a membrane hyperpolarization. However, none of the compounds was able to suppress cytokine production completely. Moreover, none of the K^+ and Cl^- channel inhibitors tested in this study exhibited significant additive inhibitory effects on IL-2 production when it was already partially inhibited by 10 nM BTP2 (Fig. 2B).

To assess the specificity of BTP2, we tested for its effects on the K^+ and Cl^- channels expressed in Jurkat cells. BTP2 did not significantly affect the activity of any of these channels, even at the highest concentration (10 μM) tested (Fig. 2C), with the possible exception of Cl^- currents, which were inhibited by ~50%. In addition, BTP2 showed no inhibitory effect on ADP-ribose-activated TRPM2 channels expressed in HEK-293 cells (Perraud et al., 2001; Sano et al., 2001) and inward rectifier K^+ currents in RBL cells (Lindau and Fernandez, 1986). Given the significant discrepancy in the potency of BTP2 to inhibit IL-2 production at low nanomolar concentrations versus I_{CRAC} inhibition with an IC_{50} value of 2.1 μM and the lack of effect on K^+ channels, we considered TRPM4, a CAN channel expressed in Jurkat cells (Launay et al., 2002, 2004), to be a possible target.

Voltage and $[Ca^{2+}]_i$ Dependence of TRPM4. We have shown previously that TRPM4 can be detected at RNA and protein levels in various T cells of murine and human origin and that these channels are functional in Jurkat T cells (Launay et al., 2004). Moreover, we have observed calcium-activated TRPM4-like currents in human primary T cells (A. Beck and R. Penner, unpublished observations). To assess TRPM4 function, we used Jurkat T cells as a model system and carried out experiments very similar to those described in Fig. 1A, except that the free Ca^{2+} concentration of the intracellular pipette solution was buffered to levels of 0.3 to 1.8 μM. Under these conditions, Jurkat cells indeed produce large cation currents with current-voltage signatures indistinguishable from those of TRPM4, and we refer to these currents as I_{CAN}. In initial experiments, application of BTP2 to maximally activated I_{CAN} did not yield any significant modification of the currents, either inhibitory or facilitatory (data not shown). However, these experiments were carried out at a holding potential of 0 mV, which yields maximal activation of I_{CAN} in Jurkat cells (Fig. 4A), whereas the resting potential of these cells is considerably more negative. The resting membrane potential is an important factor in determining TRPM4 behavior, because the channel exhibits a striking voltage dependence (Launay et al., 2002; Hofmann et al., 2003; Nilius et al., 2003). To assess the influence of membrane voltage on TRPM4 activity, we studied the voltage dependence of TRPM4 in HEK-293 cells.

Figure 3A illustrates the activation of Ca^{2+}-activated currents in TRPM4 overexpressing HEK-293 cells kept at various membrane holding potentials and perfused with a solution in which $[Ca^{2+}]_i$ was buffered to 1.3 μM. Exemplary current-voltage relationships of TRPM4 obtained by voltage ramps spanning −100 to +100 mV and delivered from holding potentials of −60 and +60 mV are illustrated in Fig. 3B. They illustrate the typical characteristics of TRPM4 as reported previously (Launay et al., 2002; Hofmann et al., 2003; Nilius et al., 2003). The data sets obtained at different holding potentials demonstrate that the magnitude of inward currents carried by TRPM4 is strongly dependent on the holding potential from which the voltage ramps are delivered. The maximum current amplitude obtained when holding the cell membrane potential at negative values is consid-

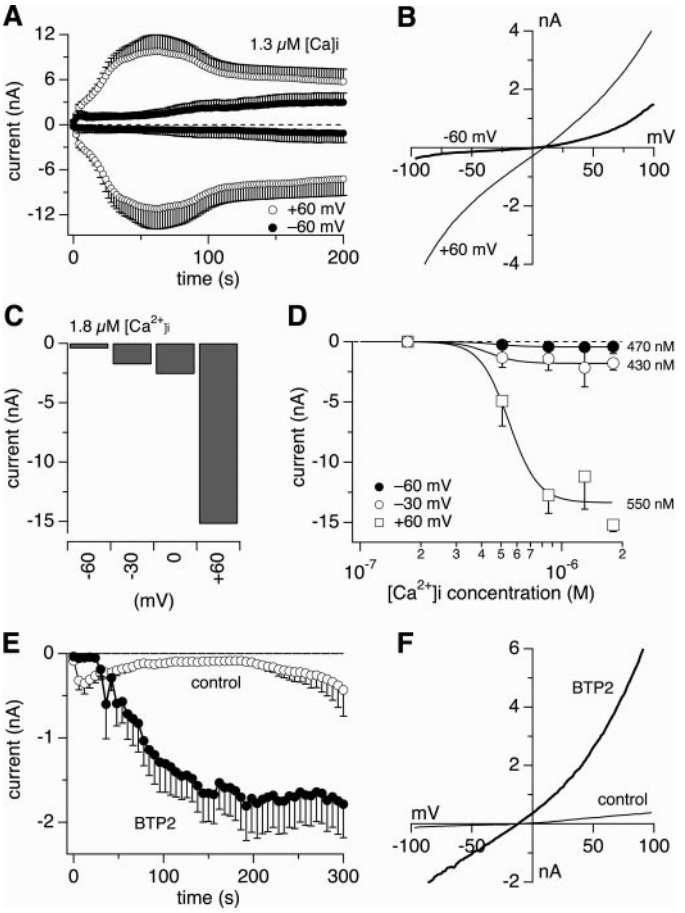

Fig. 3. Voltage dependence of TRPM4 and facilitation by BTP2. Whole-cell currents were recorded in HEK-293 cells overexpressing TRPM4. Data are ± S.E.M. where applicable. A, TRPM4 currents were activated using intracellular solutions with $[Ca^{2+}]_i$ buffered to 1.3 μM and monitored by applying voltage ramps of 50-ms duration that ranged from −100 to +100 mV from a holding potential of either −60 or +60 mV (n = 6 each). Note the strong suppression of inward currents of TRPM4 at holding potential of −60 mV. B, representative I-V relationships for TRPM4 at the two holding potentials collected 6 s after whole-cell break-in. C, average inward peak current sizes measured with 1.8 μM internal calcium and at holding potentials indicated (n = 3–6). D, dose-response curves for maximal TRPM4 inward currents at −80 mV as a function of $[Ca^{2+}]_i$ and at different holding potentials as indicated in the graph. The values at the right of each data set represent the half-maximal Ca^{2+} concentration for TRPM4 activation. Note that these values are very similar, demonstrating that the $[Ca^{2+}]_i$ dependence of TRPM4 remains unaffected by the holding potential (n = 3–6). E, average inward currents carried by TRPM4 at −80 mV with $[Ca^{2+}]_i$ clamped at 500 nM (n = 5). Control cells produce very small TRPM4 inward currents, whereas cells pretreated for 2 to 3 min with 10 μM BTP2 produce large TRPM4 currents, even at this negative holding potential (n = 5). F, current-voltage relationship under experimental conditions as in E, obtained from a representative cell 170 s after whole-cell establishment.

erably smaller than that obtained at more depolarized holding potentials (Fig. 3A). The bar graph of Fig. 3C illustrates the voltage dependence of maximum inward currents obtained by perfusing cells with 1.8 μM free Ca^{2+}.

A more comprehensive analysis of this voltage dependence is presented in Fig. 3D, in which we plot the maximum current amplitudes of TRPM4 currents (extracted from ramp currents at −80 mV) as a function of $[Ca^{2+}]_i$ and measured in cells that were held at different holding potentials (−60, −30, and +60 mV). From this analysis, it is clear that the degree of TRPM4 activation is dependent on both $[Ca^{2+}]_i$ and the membrane potential, with increasing Ca^{2+} and positive voltages synergizing to recruit larger maximal currents. The dose-response curves fitted to the various data sets of Fig. 3D reveal that the holding potential does not affect the responsiveness of TRPM4 to $[Ca^{2+}]_i$, because the apparent EC_{50} for TRPM4 activation remains fairly constant at ~500 nM, regardless of the holding potential (Fig. 3D). From this, we infer that the primary effect of membrane potential on TRPM4 activity resides at the level of the channel's open probability, which is consistent with our previous observations in single-channel recordings of TRPM4, in which negative membrane voltages strongly reduced their open probability (Launay et al., 2002).

Effect of BTP2 on TRPM4 in HEK-293 Cells. Based on the above observations, we reasoned that BTP2 could potentially increase the open probability of TRPM4 at negative membrane potentials. We therefore kept the holding potential of HEK-293 cells overexpressing TRPM4 at −80 mV and then tested BTP2 for possible augmentation of inward currents. Figure 3E illustrates the average inward currents carried by TRPM4 at −80 mV with $[Ca^{2+}]_i$ clamped at 500 nM. Control cells indeed showed a significantly reduced TRPM4 current at this negative holding potential, and these were greatly enhanced when cells were pretreated with 10 μM BTP2 for several minutes. The current-voltage relationships illustrated in Fig. 3F were obtained from representative control and BTP2-treated cells at 170 s after whole-cell establishment, and they demonstrate the massive up-regulation of TRPM4 currents by BTP2. These results suggest that BTP2 can facilitate TRPM4 channels overexpressed in the heterologous expression system.

Effect of BTP2 on I_{CAN} in Jurkat T Cells. Fig. 4A demonstrates that I_{CAN} in Jurkat cells also exhibits strong voltage dependence. Cells kept at a holding potential of 0 mV and perfused with pipette solutions in which $[Ca^{2+}]_i$ was buffered to 500 nM yielded large cation currents (Fig. 4A) with the typical current-voltage relationship of TRPM4 (Fig. 4B). Under the same experimental conditions, cells kept at a holding potential of −80 mV exhibited strongly reduced I_{CAN} current amplitudes (Fig. 4A), quite analogous to the observations made with TRPM4 in the heterologous expression system (Fig. 3A). Under these conditions, BTP2 did not enhance any currents when $[Ca^{2+}]_i$ was buffered to resting levels of 100 nM or lower (data not shown). However, when intracellular solutions were buffered to a slightly elevated $[Ca^{2+}]_i$ level of 500 nM, the preincubation of Jurkat cells with various concentrations of BTP2 resulted in a dose-dependent enhancement of Ca^{2+}-activated inward currents (Fig. 4C). The effect manifested itself in both an increase in maximal current amplitude and in the acceleration of the kinetics with which I_{CAN} developed. We analyzed the facilitation of I_{CAN} by constructing dose-response relationships for BTP2-mediated increases in inward currents as a function of BTP2 concentration 300 s after whole-cell recording (Fig. 4D). The apparent half-maximal effective concentration (EC_{50}) was 8 nM. Thus, the potency of BTP2 to enhance I_{CAN} is roughly 100-fold higher than that of inhibiting I_{CRAC} and close to its efficacy in inhibiting IL-2 production. We therefore propose that the primary action of BTP2 is based on its ability to shift the voltage dependence of TRPM4, so that open probability is increased at more negative membrane potentials. This effect enhances I_{CAN}-mediated cell membrane depolarization and thereby reduces the driving force for Ca^{2+} influx.

We sought to further corroborate the above hypothesis by

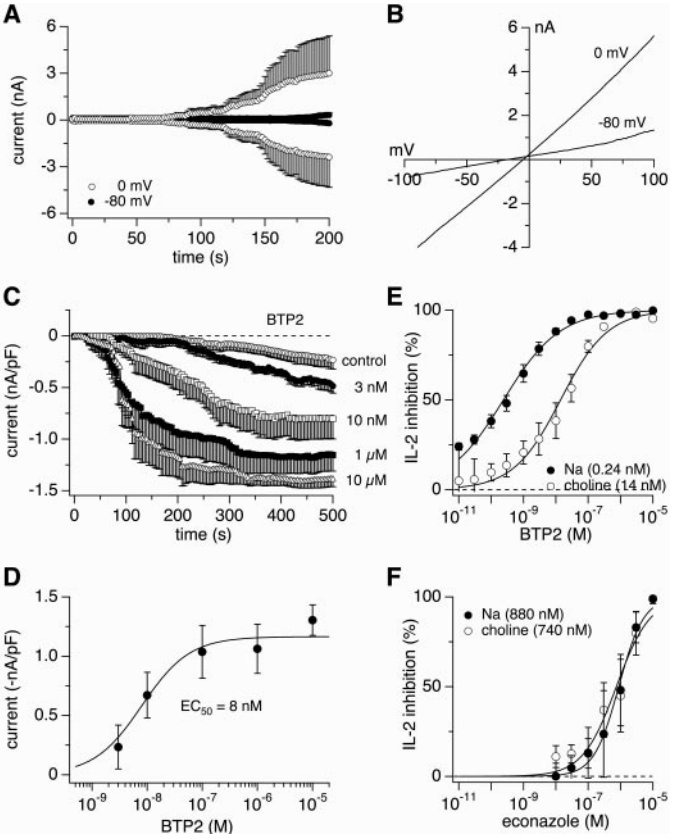

Fig. 4. Effects of BTP2 on TRPM4-like current and IL-2 production in Jurkat cells. Average whole-cell currents in Jurkat cells at −80 and +80 mV, respectively. Data are ± S.E.M. where applicable. A, TRPM4-like currents were activated using intracellular solutions with $[Ca^{2+}]_i$ buffered to 500 nM, and voltage ramps were delivered from a holding potential of either −80 or 0 mV (n = 3 each). Note the strong suppression of currents at a holding potential of −80 mV. B, representative I-V relationships for TRPM4 at the two holding potentials collected 200 s after break-in. C, average inward currents carried by TRPM4-like channels at −80 mV with $[Ca^{2+}]_i$ buffered at 500 nM in the presence of various concentrations of BTP2 (n = 10 for each set) and 0.1% dimethyl sulfoxide as a control (n = 3). D, dose-response relationship for BTP2-mediated block of TRPM4-like currents at 300 s after whole-cell establishment (K_D = 8 nM, Hill coefficient = 1). E, dose-response relationship for BTP2-mediated inhibition of IL-2 production in PHA-stimulated Jurkat cells (10 μM) assayed in either Na^+- or choline-based extracellular solutions (n = 3 each). Note the ~100-fold shift in efficacy in choline-based solution. Absolute amounts of IL-2 in Na^+-based Ringer solution were 12 ± 2 pg/ml (without PHA) and 403 ± 86 pg/ml (with 10 μg/ml PHA). Absolute amounts of IL-2 in choline-based Ringer's solution were 14 ± 3 pg/ml (without PHA) and 370 ± 67 pg/ml (with 10 μg/ml PHA). Mean ± S.E.M. F, dose-response relationship for econazole-mediated inhibition of IL-2 production in PHA-stimulated Jurkat cells (10 μM) assayed in either Na^+- or choline-based extracellular solutions (n = 3 each). Note the lack of shift in efficacy.

assessing IL-2 production in Jurkat cells under experimental conditions that would negate the depolarizing action of I_{CAN}. This can be accomplished by extracellular solutions in which Na^+, the primary charge carrier of I_{CAN}, is replaced by an impermeant cation such as choline. This largely prevents TRPM4-mediated membrane depolarization and has been shown to enhance Ca^{2+} influx (Launay et al., 2002). We analyzed the effect of BTP2 on PHA-stimulated IL-2 production in Jurkat cells cultured in the presence or absence of Na^+ in the extracellular medium. As illustrated in Fig. 4E, BTP2 potently inhibited IL-2 production in the presence of Na^+ with an IC_{50} value of 0.25 nM. This value is lower than the IC_{50} value reported previously of ~10 nM and may be a consequence of the Ringer's-like extracellular solution used in the present study. When performing the IL-2 assay in choline-based Na^+-free media under otherwise identical conditions, the IC_{50} value for BTP2-mediated inhibition of IL-2 production was reduced by approximately 100-fold (IC_{50} = 14 nM). This result is entirely consistent with the notion that at low concentrations, BTP2 acts primarily via the facilitation of I_{CAN}. The specificity of the Na^+ removal experiment is demonstrated by the dose-response curves of econazole-mediated inhibition of IL-2 production under the same experimental conditions (Fig. 4F). Here, the removal of Na^+ did not alter the efficacy of econazole to suppress cytokine production.

Discussion

Our results establish a novel principle in regulating cytokine release from lymphocytes, a process that is intimately linked to elevations in $[Ca^{2+}]_i$. We demonstrate that the pyrazole compound BTP2, a potent inhibitor of IL-2 release in lymphocytes, effectively facilitates the activity of the $[Ca^{2+}]_i$-activated nonselective cation channel TRPM4 both in a heterologous expression system and in Jurkat cells, which express the protein natively. The efficacy of facilitating I_{CAN} and the ability to suppress cytokine production occur in the low nanomolar concentration range within a few minutes of BTP2 exposure, suggesting that the primary mechanism of action of BTP2 is due to its effect on TRPM4. At higher concentrations, the compound can also inhibit I_{CRAC}. Even at these higher concentrations, the specificity of BTP2 for I_{CRAC} seems remarkable compared with the effects on a range of other ion channels found in lymphocytes. Thus, of all compounds known presently to inhibit I_{CRAC}, BTP2 represents the most potent and most selective I_{CRAC} inhibitor, even though its primary mechanism of action seems linked to TRPM4.

BTP2 seems to be a very potent inhibitor of T-cell activation in the low nanomolar range (Djuric et al., 2000; Trevillyan et al., 2001; Chen et al., 2002; Ishikawa et al., 2003); see Figs. 1 and 4), and it inhibits $[Ca^{2+}]_i$ signals within a few minutes (Fig. 1G). Any mechanism that accounts for this effect should match the potency and kinetic aspects of BTP2 action. So far, three mechanisms of BTP2 have been proposed to account for its inhibitory effects on Ca^{2+} influx and cytokine production: the inhibition of the store-operated current I_{CRAC} (Zitt et al., 2004; He et al., 2005), the inhibition of the TRPC channels TRPC3 and TRPC5b (He et al., 2005), and the facilitation of TRPM4 (the present study).

All three studies agree that store-operated Ca^{2+} influx is compromised by BTP2; however, discrepancies exist in terms of potency and kinetics of block. Zitt et al. (2004) attribute BTP2's potent suppression of Ca^{2+} influx in lymphocytes in the low nanomolar range to a slow block of I_{CRAC} that develops over hours. He et al. (2005) did not measure I_{CRAC} directly but found that thapsigargin and receptor-mediated Ca^{2+} signals were inhibited within approximately 10 min, but the potency was at least 1 order of magnitude higher (IC_{50} ~0.1–0.3 μM). It should be noted that the IC_{50} values reported by Gill and colleagues (He et al., 2005) are not directly comparable with the values provided by Zitt et al. (2004) or our own study, because they represent only indirect measures of channel activity as determined from changes in $[Ca^{2+}]_i$ and therefore probably overestimate the true potency at the channel level. Our study finds that I_{CRAC} in RBL and Jurkat T cells can indeed be inhibited relatively quickly within a few minutes, and potencies range from 0.5 to 4 μM as derived from direct current inhibition profiles. Whereas the study of Zitt et al. (2004) is compatible with the potency range of BTP2 on inhibition of cytokine production, the slow kinetics of I_{CRAC} inhibition reported by Zitt et al. (2004) is at odds with the relatively fast inhibition of Ca^{2+} influx (Fig. 1G). Conversely, the studies by He et al. (2005) and our own data are compatible with the kinetics of inhibition of store-operated currents, but neither study found a low nanomolar potency that would be required to explain the efficacy of BTP2 in terms of I_{CRAC} inhibition alone. Likewise, the efficacy of BTP2 in blocking other channels such as heterologously expressed TRPC3 and TRPC5, which He et al. (2005) estimate to be ~0.3 μM, does not approach the low BTP2 concentrations that suffice to mediate the inhibition of cytokine release in native T cells. These channels also would not seem to be responsible for BTP-mediated inhibition of cytokine release from lymphocytes, because the only Ca^{2+}-permeable current elicited by either antigen or thapsigargin stimulation seems to be I_{CRAC}, and no ion channels that fit the profile of TRPC3 or TRPC5 have so far been reported in the literature. From these considerations and based on the data present in this study, it seems that the only mechanism which fits the criteria for BTP2 effects in T cells in terms of potency and kinetics is provided by the facilitation of TRPM4. Not only are the potency and kinetic properties adequate, but these channels have been identified in T cells as important factors in determining the amount of Ca^{2+} influx (Launay et al., 2004). At higher concentrations, I_{CRAC} inhibition may contribute to this inhibition. Likewise, at these higher concentrations and in cell types that express TRPC3/TRPC5, the BTP2 effects may also involve inhibition of TRPC channels.

Acknowledgments

We thank Mahealani K. Monteilh-Zoller and Carolyn E. Oki for expert technical assistance.

References

Bodding M (2001) Reduced store-operated Ca^{2+} currents in rat basophilic leukaemia cells cultured under serum-free conditions. *Cell Calcium* **30:**141–150.
Cahalan MD and Chandy KG (1997) Ion channels in the immune system as targets for immunosuppression. *Curr Opin Biotechnol* **8:**749–756.
Cahalan MD, Wulff H, and Chandy KG (2001) Molecular properties and physiological roles of ion channels in the immune system. *J Clin Immunol* **21:**235–252.
Chen Y, Smith ML, Chiou GX, Ballaron S, Sheets MP, Gubbins E, Warrior U, Wilkins J, Surowy C, Nakane M, et al. (2002) TH1 and TH2 cytokine inhibition by 3,5-bis(trifluoromethyl)pyrazoles, a novel class of immunomodulators. *Cell Immunol* **220:**134–142.
Christian EP, Spence KT, Togo JA, Dargis PG, and Warawa E (1996) Extracellular

site for econazole-mediated block of Ca^{2+} release-activated Ca^{2+} current I_{CRAC} in T lymphocytes. *Br J Pharmacol* **119:**647–654.
Chung SC, McDonald TV, and Gardner P (1994) Inhibition by SK&F 96365 of Ca^{2+} current, IL-2 production and activation in T lymphocytes. *Br J Pharmacol* **113:** 861–868.
Clapham DE, Runnels LW, and Strubing C (2001) The TRP ion channel family. *Nat Rev Neurosci* **2:**387–396.
Desai R, Peretz A, Idelson H, Lazarovici P, and Attali B (2000) Ca^{2+}-activated K^+ channels in human leukemic Jurkat T cells. Molecular cloning, biochemical and functional characterization. *J Biol Chem* **275:**39954–39963.
Djuric SW, BaMaung NY, Basha A, Liu H, Luly JR, Madar DJ, Sciotti RJ, Tu NP, Wagenaar FL, Wiedeman PE, et al. (2000) 3,5-Bis(trifluoromethyl)pyrazoles: a novel class of NFAT transcription factor regulator. *J Med Chem* **43:**2975–2981.
Franzius D, Hoth M, and Penner R (1994) Non-specific effects of calcium entry antagonists in mast cells. *Pflueg Arch Eur J Physiol* **428:**433–438.
Hanson DC, Nguyen A, Mather RJ, Rauer H, Koch K, Burgess LE, Rizzi JP, Donovan CB, Bruns MJ, Canniff PC, et al. (1999) UK-78,282, a novel piperidine compound that potently blocks the Kv1.3 voltage-gated potassium channel and inhibits human T cell activation. *Br J Pharmacol* **126:**1707–1716.
Harteneck C, Plant TD, and Schultz G (2000) From worm to man: three subfamilies of TRP channels. *Trends Neurosci* **23:**159–166.
He LP, Hewavitharana T, Soboloff J, Spassova MA, and Gill DL (2005) A functional link between store-operated and TRPC channels revealed by the 3,5-bis(trifluoromethyl)pyrazole derivative, BTP2. *J Biol Chem* **280:**10997–11006.
Hermosura MC, Monteilh-Zoller MK, Scharenberg AM, Penner R, and Fleig A (2002) Dissociation of the store-operated calcium current I_{CRAC} and the Mg-nucleotide-regulated metal ion current MagNuM. *J Physiol* **539:**445–458.
Hofmann T, Chubanov V, Gudermann T, and Montell C (2003) TRPM5 is a voltage-modulated and Ca^{2+}-activated monovalent selective cation channel. *Curr Biol* **13:**1153–1158.
Hoth M and Penner R (1992) Depletion of intracellular calcium stores activates a calcium current in mast cells. *Nature (Lond)* **355:**353–356.
Hoth M and Penner R (1993) Calcium release-activated calcium current in rat mast cells. *J Physiol* **465:**359–386.
Ishikawa J, Ohga K, Yoshino T, Takezawa R, Ichikawa A, Kubota H, and Yamada T (2003) A pyrazole derivative, YM-58483, potently inhibits store-operated sustained Ca^{2+} influx and IL-2 production in T lymphocytes. *J Immunol* **170:**4441–4449.
Jensen BS, Odum N, Jorgensen NK, Christophersen P, and Olesen SP (1999) Inhibition of T cell proliferation by selective block of Ca^{2+}-activated K^+ channels. *Proc Natl Acad Sci USA* **96:**10917–10921.
Launay P, Cheng H, Srivatsan S, Penner R, Fleig A, and Kinet J-P (2004) TRPM4 regulates calcium oscillations after T cell activation. *Science (Wash DC)* **306:**1374–1377.
Launay P, Fleig A, Perraud AL, Scharenberg AM, Penner R, and Kinet JP (2002) TRPM4 is a Ca^{2+}-activated nonselective cation channel mediating cell membrane depolarization. *Cell* **109:**397–407.
Lewis RS, Ross PE, and Cahalan MD (1993) Chloride channels activated by osmotic stress in T lymphocytes. *J Gen Physiol* **101:**801–826.
Lin CS, Boltz RC, Blake JT, Nguyen M, Talento A, Fischer PA, Springer MS, Sigal NH, Slaughter RS, Garcia ML, et al. (1993) Voltage-gated potassium channels regulate calcium-dependent pathways involved in human T lymphocyte activation. *J Exp Med* **177:**637–645.
Lindau M and Fernandez JM (1986) A patch-clamp study of histamine-secreting cells. *J Gen Physiol* **88:**349–368.
Mason MJ, Mayer B, and Hymel LJ (1993) Inhibition of Ca^{2+} transport pathways in thymic lymphocytes by econazole, miconazole and SKF 96365. *Am J Physiol* **264:**C654–C662.
Montell C, Birnbaumer L, and Flockerzi V (2002a) The TRP channels, a remarkably functional family. *Cell* **108:**595–598.
Montell C, Birnbaumer L, Flockerzi V, Bindels RJ, Bruford EA, Caterina MJ, Clapham DE, Harteneck C, Heller S, Julius D, et al. (2002b) A unified nomenclature for the superfamily of TRP cation channels. *Mol Cell* **9:**229–231.
Nilius B, Prenen J, Droogmans G, Voets T, Vennekens R, Freichel M, Wissenbach U, and Flockerzi V (2003) Voltage dependence of the Ca^{2+}-activated cation channel TRPM4. *J Biol Chem* **278:**30813–30820.
Parekh AB and Penner R (1997) Store depletion and calcium influx. *Physiol Rev* **77:**901–930.
Penner R, Fasolato C, and Hoth M (1993) Calcium influx and its control by calcium release. *Curr Opin Neurobiol* **3:**368–374.
Penner R, Matthews G, and Neher E (1988) Regulation of calcium influx by second messengers in rat mast cells. *Nature (Lond)* **334:**499–504.
Perraud AL, Fleig A, Dunn CA, Bagley LA, Launay P, Schmitz C, Stokes AJ, Zhu Q, Bessman MJ, Penner R, et al. (2001) ADP-ribose gating of the calcium-permeable LTRPC2 channel revealed by Nudix motif homology. *Nature (Lond)* **411:**595–599.
Premack BA, McDonald TV, and Gardner P (1994) Activation of Ca^{2+} current in Jurkat T cells following the depletion of Ca^{2+} stores by microsomal Ca^{2+}-ATPase inhibitors. *J Immunol* **152:**5226–5240.
Putney JW Jr, Broad LM, Braun FJ, Lievremont JP, and Bird GS (2001) Mechanisms of capacitative calcium entry. *J Cell Sci* **114:**2223–2229.
Ross PE, Garber SS, and Cahalan MD (1994) Membrane chloride conductance and capacitance in Jurkat T lymphocytes during osmotic swelling. *Biophys J* **66:**169–178.
Sano Y, Inamura K, Miyake A, Mochizuki S, Yokoi H, Matsushime H, and Furuichi K (2001) Immunocyte Ca^{2+} influx system mediated by LTRPC2. *Science (Wash DC)* **293:**1327–1330.
Trevillyan JM, Chiou XG, Chen YW, Ballaron SJ, Sheets MP, Smith ML, Wiedeman PE, Warrior U, Wilkins J, Gubbins EJ, et al. (2001) Potent inhibition of NFAT activation and T cell cytokine production by novel low molecular weight pyrazole compounds. *J Biol Chem* **276:**48118–48126.
Wulff H, Miller MJ, Hansel W, Grissmer S, Cahalan MD, and Chandy KG (2000) Design of a potent and selective inhibitor of the intermediate-conductance Ca^{2+}-activated K^+ channel, IKCa1: a potential immunosuppressant. *Proc Natl Acad Sci USA* **97:**8151–8156.
Zitt C, Strauss B, Schwarz EC, Spaeth N, Rast G, Hatzelmann A, and Hoth M (2004) Potent inhibition of Ca^{2+} release-activated Ca^{2+} channels and T-lymphocyte activation by the pyrazole derivative BTP2. *J Biol Chem* **279:**12427–12437.
Zweifach A and Lewis RS (1993) Mitogen-regulated Ca^{2+} current of T lymphocytes is activated by depletion of intracellular Ca^{2+} stores. *Proc Natl Acad Sci USA* **90:**6295–6299.

Address correspondence to: Dr. Reinhold Penner, Center for Biomedical Research, The Queen's Medical Center, 1301 Punchbowl St., UHT 8, Honolulu, HI 96813. E-mail: rpenner@hawaii.edu